A calibrated UV LED light source for photocatalytic experimentation

A. Sergejevs[1], C. T. Clarke[1], D. Allsopp[1], J. Marugan[2], and C. Bowen[1]
1. University of Bath, Bath, United Kingdom 2. Universidad Rey Juan Carlos, Madrid, Spain

***Abstract*— Photocatalysis is an evolving field that has a potential to become a cost effective water cleaning method. One of the most studied photocatalysts is Titanium Dioxide (TiO_2). It has a high activity in response to UV wavelengths but almost no activity in the visible region of the spectrum. The activity changes rapidly between roughly 340 and 370 nm although this can be modified by doping. This region of the spectrum corresponds to the current lower limit of high efficiency LEDs. This presents a challenge in the use of UV LEDs for commercially viable photocatalysis and makes accurate comparisons of experimental data between different research groups essential. This paper presents a photocatalytic test reactor that provides a calibrated light source and pre-defined test conditions to remove as many sources of uncertainty as possible to improve data comparability. The test reactor provides a selectable intensity of up to 1.9 kW/m^2 at the photocatalyst surface. The comparability of the results is achieved through the use of pre-calibration and control electronics that minimizes the biggest source of uncertainty – intensity variation between individual LEDs. The system devised reduces the intensity variation between systems by a factor of 11.6.**

***Index Terms*—Chemical Reactors, FPGA, LED, Materials Testing, Photocatalysis**

I. Introduction

PHOTOCATALYSTS require energy provided by light within a specific wavelength range to initiate a chemical reaction. When excited by light with the energy equal or greater than the semiconductor band gap of the photocatalyst, electron-hole pairs are produced at the surface. Once generated, these electron-hole pairs initiate reduction and oxidation (redox) reactions [1]. These reactions exhibit properties required in some fields, for example in organic waste from water removal [2]. During these reactions organic pollutants undergo changes and are degraded to their intermediate products and subsequently further mineralized to innocuous carbon dioxide.

One of the most studied photocatalysts is Titanium Dioxide (TiO_2), mainly due to its properties such as non-toxicity and stability [2]. In the case of pure TiO_2, ultraviolet light of a specific wavelength range (≤ 370 nm) is required for a chemical reaction to happen [1]. Absorption characteristics of pure TiO_2 suggest that light with the wavelength shorter than ~365 nm will result in the best performance of the semiconductor [3]. There are light sources that would radiate at such wavelength range, but their low efficiency makes them an undesired choice for the use with photocatalysts.

The most commonly used Ultra Violet (UV) light source is mercury gas discharge lamp. It has multiple spectral components in the UV region of the spectrum as well as spectral components in the visible portion of the spectrum [4]. The fact that there are multiple UV spectral components makes mercury gas lamps an unsuitable light source for the photocatalytic experimentation since it may not be clear which spectral component is responsible for activation.

Light Emitting Diodes (LEDs) can be used as an alternative to the mercury gas lamps. LEDs radiate at a single dominant wavelength with a relatively narrow spectral spread, usually around 50 nm. Although there are some LEDs that radiate at dominant wavelengths shorter than 365 nm, the efficiency of such LEDs is very low (for example 0.78% at 0.28W of electrical power consumption for a Roithner Laser Technik 340nm LED [5]). Although more energy per nm is provided to TiO_2, the light output of these LEDs is too low to offset the improvements in the photocatalytic performance of TiO_2 compared to recently developed innovative 365 nm high brightness LEDs (for example 30% at 3W of electrical power consumption for LEDEngin 365nm LED [6]) .

In order to achieve comparable results from the experiments with TiO_2 the evenness of the light distribution across the photocatalytic sample has to be considered. TiO_2 is usually used in powder form and is dispersed in the liquid. This makes it hard to estimate the surface area of the sample. In this work the TiO_2 samples used were manufactured in the form of disks with the diameter of 40 mm. Such form of the sample is chosen for a better estimate of the area and allows a controlled positioning of the sample with respect to the light source. As a result a more even distribution of light across the sample surface with known intensity can be achieved.

In this paper the UV lighting system for the photocatalytic experimentation as part of the PCATDES project is presented. It consists of the light source, light source controller, photocatalytic reactor and a cooling system. The light source consists of UV LEDs that are split into individually controlled

PCATDES receives funding from European Union's Seventh Framework Programme under Grant Agreement N. 309846

groups (channels). Such splitting allows the adjustment of intensity for achieving desired light radiation patterns. Each LED channel has its own controller (driver) that controls the input power to the channel thus controlling the intensity. Higher input power results in higher heating of the LEDs since only ~30% of that power is converted to the UV light with remaining power being converted to heat. The liquid cooling system is responsible for removing the excess heat from the LEDs allowing them to operate in optimal conditions. Heat management of LEDs is essential since the rise in the device temperature will cause the drop in intensity and red shift in wavelength.

The sample disk is placed into the reactor holder that is fixed to the lid and submerged into the water. The light source is placed in the lid at a fixed distance from the photocatalytic sample. Such an arrangement allows comparable results from different experiments to be achieved by ensuring that the sample and the light source are always separated by the same distance.

A. Contributions

This paper describes the following contributions to lighting equipment for photocatalytic experimentation:

1. UV light source with narrow spectral spread. Narrow spread allows for the achievement of better results by eliminating interference from other spectral components in, for example, mercury gas lamps.
2. The light source described in this paper provides the ability to control the intensity of the UV light to achieve better control of experiments.
3. The light output of the LEDs used increases the UV power density significantly over previously reported systems [9-11]. Power at the surface of the photocatalytic sample is ~2.4 W. This is equivalent to ~1.9 kW/m^2 of 360-370nm UV.

II. System Description

The system consists of multiple parts. They will be described in this section.

A. UV Light Generation

UV light is generated by the LEDs that are arranged into channels with each channel consisting of 3 LEDs. Each channel is controlled individually by adjusting the electrical power delivered to that channel. The power is delivered in the form of Pulse-Width Modulated (PWM) waveform. The PWM duty cycle controls the average intensity of the LEDs.

B. LED Intensity Control

PWM signal is generated by an LED driver. Each channel has its own driver. The driver includes monitors for voltage and current supplied to LEDs for the fault detection and feedback. There is also a temperature monitor on the driver for circuitry overheating protection. Another overheating prevention mechanism is the heatsink that is located on the other side of the driver's PCB. It is a forced convection heatsink; the air flow is created by the means of 2 fans in the control electronics' enclosure.

C. Photocatalytic Reactor

The photocatalytic reactor shown in Fig 1. is a glass vessel for the liquid sample. Its walls are made hollow to allow the use of liquid cooling of the sample. The vessel is surrounded by a plastic enclosure for the purposes of safety. The lid of the enclosure holds the UV LED array and has a photocatalyst disk holder. Once the lid is installed on the enclosure, the photocatalyst holder is submerged into the liquid. The LED array is located at a distance of 10 cm from the photocatalyst.

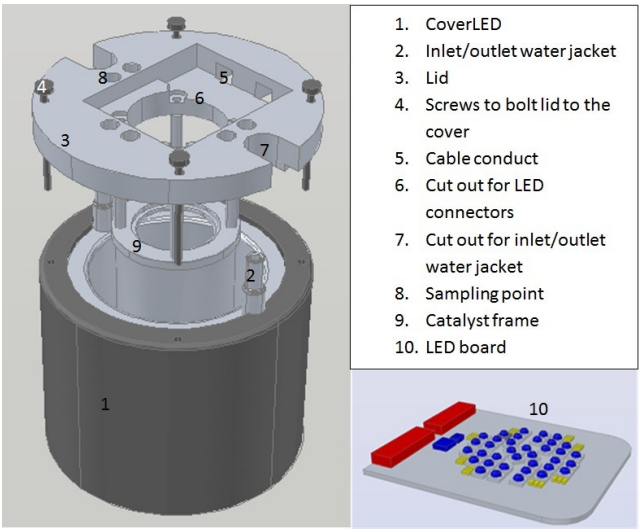

Fig. 1. Schematic diagram of the photocatalytic reactor.

Reactor lid also has 6 sampling holes that can be used for pH or temperature monitoring or for extracting water samples during the experiment.

III. LED Board

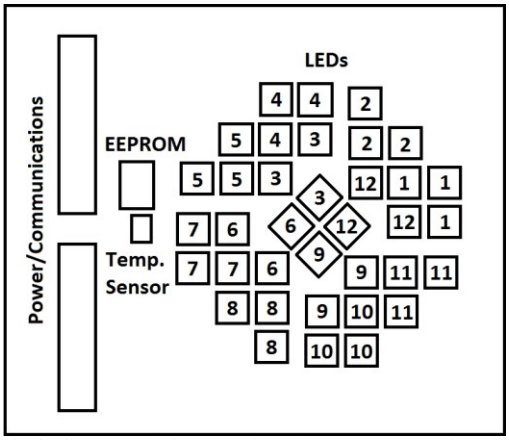

Fig. 2. Block diagram of the LED board. LEDs are numbered in groups showing which channel they belong to.

There are 36 LEDs on the LED board controlled in 12 individual channels. Each channel consists of a group of 3 LEDs wired in series. The arrangement of LEDs shown in Fig. 2 is designed to provide the best illumination of the photocatalytic sample that is a disk of 40 mm diameter. The board is an Insulated Metal Substrate (IMS) PCB for better thermal management. Each LED outputs 800 mW of optical power over its radiation pattern when driven at full electrical

power. This corresponds to 116 mW of UV in the direction of the sample (near field), which results in ~2.4 W of UV on the surface of the sample (far field). This amount of power corresponds to the ~1.9 kW/m^2 of optical power at the distance of 0.1 m from the LEDs.

There is a ±10% variation in optical power between LEDs, as well as ±2 nm variation in dominant wavelength [6]. In order to achieve a better control of the optical power delivered to the sample, an Electrically Erasable Programmable Read-Only Memory (EEPROM) chip is added to the LED light source. The EEPROM holds calibration information that is used to estimate the intensity of each channel at different electrical power levels and the information on dominant wavelength offset from the desired (365 nm). Using this information and the fact that LED channels have individual drivers, the controller is able to adjust the input power to any channel so that all channels provide the same optical power. Placement of the EEPROM chip on the LED board ensures that the calibration information stays with the light source. This allows the UV light source to be used with a different controller while maintaining the same performance.

Since LEDs are heat sensitive, a temperature sensor is placed on the PCB of the UV light source. The sensor is used as an overheating protection. If the temperature of the PCB reaches a certain pre-defined value, the electrical power to the LEDs will be switched off.

IV. Control Of UV Light Source

LEDs are controlled with the PWM signal generated by the LED driver circuitry. This signal is created by Texas Instruments LM3405 LED driver chip, that is capable of providing 1 A of current at up to 22 V [7]. The LM3405 chip is incorporated into a custom PCB with additional circuitry and sensors.

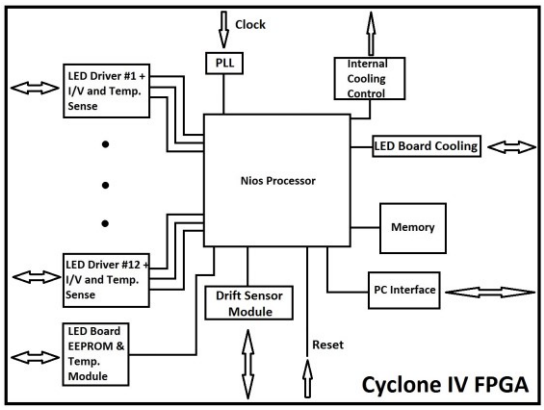

Fig. 3. Block diagram of the FPGA showing NIOS processor and its modules.

The LM3405 is driven by a PWM signal from the Field Programmable Gate Array (FPGA) that is used as a main controller for the system. The PWM signal generated by the FPGA acts as a trigger for the LM3405, since FPGA is not capable of providing enough power to drive LEDs. The intensity of LEDs is controlled by adjusting the duty cycle of the PWM signal generated by the FPGA. Switching frequency of the LM3405 is fixed at 1.6 MHz [7].

The FPGA has a NIOS processor implemented as digital hardware. This processor is responsible for the control of the system and data acquisition from the sensors as shown in Fig. 3.

The NIOS processor constantly monitors the state of the sensors on the LED board and LED drivers. If a fault has been detected, the processor will turn off LEDs and inform the user about the detected fault. Such feedback is provided through the PC software and through the indicator LEDs on the front panel of the control electronics' enclosure. It also controls both cooling systems, LED and driver cooling. The control of LED cooling system is achieved through the control of a digital potentiometer that mimics the behavior of the thermistor.

The NIOS process is also responsible for data acquisition from the drift sensor board. The data is acquired by addressing each individual sensor on the drift board via I^{2}C communications.

V. Drift Sensor

During extended use, some of the characteristics of LEDs, such as intensity and wavelength, may change. Changes in those characteristics will affect the outcome of experiments. In order to check that LED characteristics have not changed significantly, a drift sensor was created. This sensor consists of 12 Avago Technologies APDS-9301-020 miniature ambient light sensors. These sensors have 2 photodiodes, each one with a different spectral response. The sensor communicates with the control electronics via I^{2}C communications protocol.

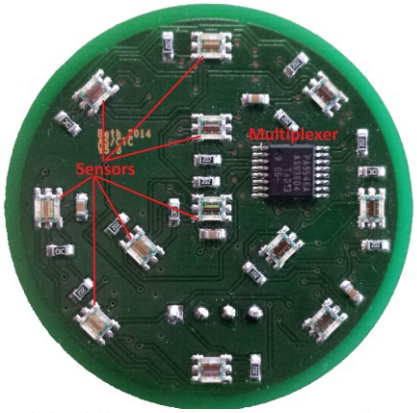

Fig. 4. Photo of the drift sensor board. Sensors are located as evenly as possible across the board.

The drift sensor is made in the form of a disk as shown in Fig. 4 in order to fit into the sample holder. It has a diameter that is marginally smaller than that of a photocatalytic sample, 39 mm instead of 40 mm. This allows easier positioning and removal of the drift sensor in the sample holder.

The drift sensor provides a relative measurement of the LED intensity. Its main uses are checks of relative LED intensity and uniformity of light distribution and acquisition of the

calibration data that is later stored on the EEPROM of the LED board. The drift sensor can also be used for recalibration of the system that can be performed by the user.

VI. Potential Sources of Error

The performance of the system was tested by checking the intensity differences between LED channels after the characterization and evenness of the UV light distribution at a distance of 10 cm from the LEDs. The drift sensor described in this paper was used for both of these tasks, as well as for the characterization of LED intensities.

The characterization information was acquired by turning each LED channel in turn at a set duty cycle and recording 10 readings from all sensors on the drift board. The average of those readings was calculated for each channel and compared against other channels on the LED board. All readings are relative since sensors used are unable to provide a measure of true optical power (absolute irradiance) from LEDs.

After the average intensity of all channels was found, first correction factor for each channel is calculated. This factor takes into account the relative position of LEDs in the channel to each individual sensor on the drift sensor board. Angular response of sensors [8] and radiation pattern of LEDs [6] are used to calculate this factor.

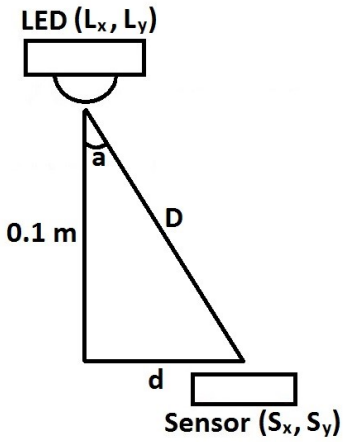

Fig. 5. Schematic of relative positions between LED and individual sensors.

Once the first correction factors are obtained, they are applied to appropriate channels. This produces an array of true relative intensities at given requested intensities. This information is then used to calculate a quadratic line of best fit for each LED channel. These equations are then used by the control electronics to adjust the current to LEDs based on the user requested intensity.

VII. Results

LED intensity is adjusted according to the data stored in the EEPROM. The data for the intensity corrections is expressed as the 3 coefficients for a quadratic equation. The equation is of a line of best fit for the processed intensity measurements. The quadratic form is chosen due to lack of space on the EEPROM to store more coefficients for all 12 channels. When an intensity level is requested by the user, NIOS uses the coefficients from the EEPROM to calculate the amount of current that needs to be passed to a given channel. Such corrections to the LED intensity give users more control of the experiments and produce more reliable experimental results.

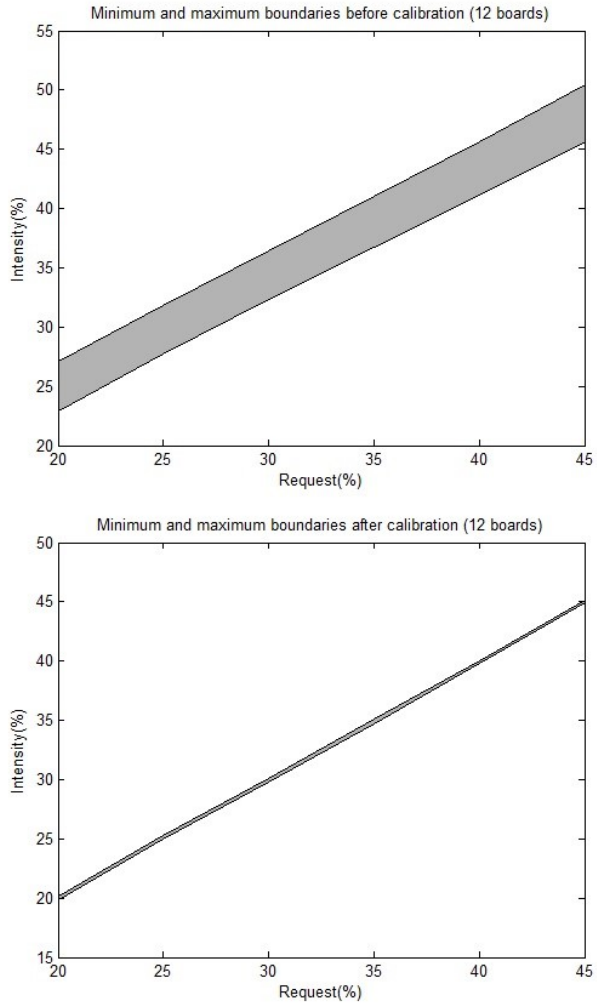

Fig. 6. Comparison of LED intensity output before (measured) (top) and after (predicted) (bottom) calibration. Top graph shows a region between minimum and maximum intensities achieved at given requested intensities. Line of best fit was constructed for each channel using the uncalibrated data seen on the top graph.

Use of the quadratic line of best fit for calibration resulted in improved intensity output at given requested intensity. The predicted output intensity at any given requested intensity has become more linear. The data is matched to the weakest channel across all LED boards so that all systems have the same performance range as each other.

Uncalibrated intensity error with respect to the expected user requested optical output is shown in Fig 7. The errors form of a Gaussian distribution which is to be expected from a relatively large population size (over 1000 points). The modal channel error is 3.5% from the requested intensity value, with a maximum of 6.5%. Although the variation in intensity between individual LEDs can be as high as 10%, grouping LEDs into channels with 3 devices may have had the effect of reducing the typical variation.

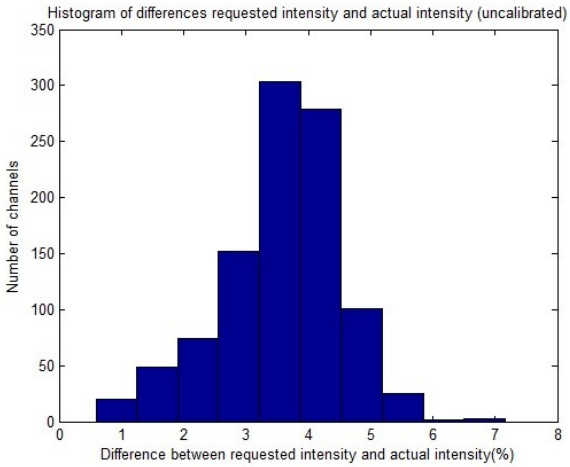

Fig. 7. Histogram of the differences between requested intensity and actual measured intensity. There are no channels below zero as channel with lowest intensity is set as the zero reference.

After the calibration is applied the error between user requested intensity and system output intensity (predicted) is significantly reduced. The largest predicted intensity error is 1.8% due to non-linearities in the response of one LED in the test sample. Overall, predicted intensity values lie within 0.5% region from expected.

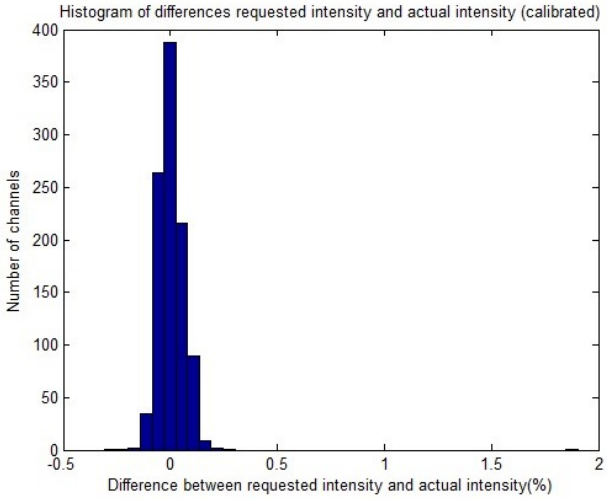

Fig. 8. Histogram of the differences between requested intensity and predicted intensity after applying calibration.

The calibration information stored on the EEPROM also includes the wavelength offset from nominal for each LED channel. This information is valuable for users whose experiments are strongly dependant on the wavelength. It allows the user to calculate the output spectrum of light in the system and correct for spectral variations if necessary.

VIII. Conclusion

UV LEDs have the potential to provide a rugged and high efficiency light source for photocatalytic water treatment. However, comparisons between experiments using UV LEDs as a light source are prone to error due to variation in individual LED characteristics in use, differences in LED performance due to manufacturing process variability and improvements in the manufacturing processes over time.

This paper has demonstrated an effective methodology to reduce the variation of light output from a high power UV light source through the use of pre-calibration which can be repeated to account for the effects of ageing on the LEDs. The calibration process allows the user to be certain that the requested intensity value will be very close to the actual intensity of all LED channels. The predicted behavior of the LEDs after calibration has demonstrated 11.6 times reduction in output intensity spread when compared with uncalibrated data. The described system has been delivered to PCATDES project partners and is currently being used for photocatalytic experimentation and comparison of results.

IX. Acknowledgements

The authors would like to express their thanks to their research colleagues working on the PCATDES project and to the European Commission. PCATDES receives funding from European Union's Seventh Framework Programme under Grant Agreement N. 309846

References

[1] M. M. Haque, D. Bahnemann, M. Muneer, "Photocatalytic Degradation of Organic Pollutants: Mechanisms and Kinetics," in *Organic Pollutants Ten Years After the Stockholm Convention – Environmental and Analytical Update,* Rijeka, Croatia: InTech, 2012, ch. *12*, sec. *3*, pp. *293-326.*

[2] M. N. Chong, B. Jin, C. W. K. Chow, C. Saint, "Recent Developments in Photocatalytic Water Treatment Technology: A Review,": http://publicationslist.org/data/meng.chong/ref-18/sdarticle.pdf

[3] K. Dai, L. Lu, G. Dawson, "Development of UV-LED-TiO_2 Device and their Application for Photocatalytic Degradation of Methylene Blue," http://www.mdpi.com/2073-4344/3/3/726/pdf

[4] http://www.cairnweb.com/manuals/specman/lightsource.html

[5] http://www.roithner-laser.com/datasheets/led_deepuv/duv-sml.pdf

[6] http://www.ledengin.com/files/products/LZ1/LZ1-00UV00.pdf

[7] http://www.farnell.com/datasheets/1676919.pdf

[8] http://www.farnell.com/datasheets/1816958.pdf

[9] http://ntrs.nasa.gov/archive/nasa/casi.ntrs.nasa.gov/20110011605.pdf

[10] http://ieeexplore.ieee.org/stamp/stamp.jsp?tp=&arnumber=7116957

[11] http://ac.els-cdn.com/S0196890416301236/1-s2.0-S0196890416301236-main.pdf?_tid=a7959716-fd99-11e5-a0e3-00000aab0f27&acdnat=1460127388_e025f0394d6141d8ab918add8c1d6662